Lagrangian Sharp Interface Schemes for Multimaterials

T. Milcent [a,*], A. Iollo [b]

[a] I2M and Arts et Métiers Paristech, Bordeaux - France
16 avenue Pey-Berland, 33607 Pessac Cedex

[b] IMB and Inria, Bordeaux - France
351 cours de la liberation, 33405 Talence Cedex

*thomas.milcent@u-bordeaux1.fr

Abstract. *We present multi-material simulations in the Lagrangian framework. The methods employed are based on classical Godunov-like methods that are adapted to treat the case of interfaces separating different materials. In the models considered the gas, liquids or elastic materials are described by specific constitutive laws, but the governing equations are the same. Examples of gas-gas and elastic-elastic material interactions are presented.*

Keywords: compressible multimaterial, lagrangian elasticity, hllc riemann solver

1 INTRODUCTION

Physical and engineering problems that involve several materials are ubiquitous in nature and in applications. The main contributions in the direction of simulating these phenomena go back to [1] for the model and [2] for numerical simulations. However, the numerical scheme presented in that paper is relatively complicated and has the disadvantage that the interface is diffused over a certain number of grid points. We have already developed a numerical scheme for multimaterial in the Eulerian context. The scheme is based on a directional splitting on a fixed cartesian mesh where the fluxes are computed by an HLLC approximate Riemann solver. The interface is kept sharp by using a non-conservative numerical flux and the numerical solution is stable and non-oscillating. We refer for the numerical results to [3] and [4]. This paper is devoted to the extension this method in the Lagrangian framework.

2 LAGRANGIAN MODEL

The conservative form of elastic media equation in the Lagrangian framework are

$$
\begin{cases}
(\rho_0 u)_t - \mathrm{div}_\xi(\mathcal{T}) = 0 \\
(\nabla_\xi X)_t - \nabla_\xi u = 0 \\
(\rho_0 e)_t - \mathrm{div}_\xi(\mathcal{T}^T X_t) = 0
\end{cases}
\tag{1}
$$

The unknowns are the velocity $u(\xi, t)$, the gradient of the direct characteristics $\nabla_\xi X(\xi, t)$ and the total energy per unit mass $e(\xi, t)$. Here $\mathcal{T}(\xi, t)$ is the first Piola-Kirchoff stress tensor in the reference domain and $\rho_0(\xi)$ is the initial density.

To close the system, a constitutive law is chosen (ε is the internal energy per unit mass)

$$
\varepsilon = e - \frac{1}{2}|u|^2 = \frac{\exp\left(\frac{s}{c_v}\right)\rho^{\gamma-1}}{\gamma-1} + \frac{p_\infty}{\rho} + \frac{\chi}{\rho_0}(\mathrm{Tr}(\overline{C}) - 2)
\tag{2}
$$

where s is the entropy, $J = \det(\nabla_\xi X)$ is the volume ratio, $\rho = \rho_0/J$ is the density, and $\overline{C} = [\nabla_\xi X]^T[\nabla_\xi X]/J$ is the modified right Cauchy-Green tensor. The constants $c_v, \gamma, p_\infty, \chi$ characterize a given material. The two first

terms of (2) represent a stiffened gas and the third one represents a Neo-Hookean elastic solid. The stress tensors $\mathcal{T}$ is then derived from this constitutive law as a function of the problem unknowns.

3 NUMERICAL SCHEME

Let $x = (x_1, x_2)$ be the coordinates in the canonical basis of $\mathbb{R}^2$, $u = (u_1, u_2)$ the velocity components, $X = (X^1, X^2)$ the components of X and $\mathcal{T}^{ij}$ the components of the stress tensor $\mathcal{T}$. Also, let us denote by $, i$ differentiation with respect to x_i. Our scheme is based on a directional splitting on a cartesian mesh. When computing the numerical fluxes at cell interfaces in the x_1 direction we have $(X^1_{,2})_t = (X^2_{,2})_t = 0$ thus $X^1_{,2}$ and $X^2_{,2}$ are constants. The governing equations in conservative form become

$$\Psi_t + (F(\Psi))_{,1} = 0 \tag{3}$$

where

$$\Psi = \begin{pmatrix} \rho_0 u_1 \\ \rho_0 u_2 \\ X^1_{,1} \\ X^2_{,1} \\ \rho_0 e \end{pmatrix} \qquad F(\Psi) = \begin{pmatrix} -\mathcal{T}^{11} \\ -\mathcal{T}^{21} \\ -u_1 \\ -u_2 \\ -\mathcal{T}^{11} u_1 - \mathcal{T}^{21} u_2 \end{pmatrix} \tag{4}$$

We use a classical finite volume method to integrate the equation (3) with first order accuracy in time and space and the numerical fluxes are computed with a HLLC approximate Riemann solver. Let Ψ_l and Ψ_r denote the left and right states of the Riemann problem. The wave pattern involves five waves (the waves speeds are the eigenvalues of $F'(\Psi)$) in the exact problem but the HLLC approximate solver approaches the solution using three waves (the fastest waves velocities s_l, s_r and the contact discontinuity which is zero in the Lagrangian framework) and thus defining two intermediate states Ψ^+ and Ψ^- (see Figure 1). The HLLC scheme is based on the assumption that every wave is a shock and thus Rankine Hugoniot relations are used to determine the two intermediate states.
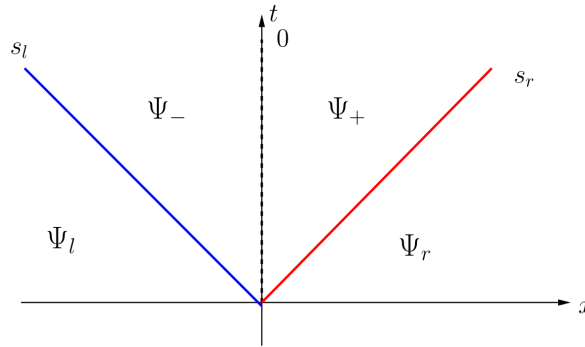

Figure 1: HLLC solver wave pattern

4 NUMERICAL RESULTS

4.1 1D results

The numerical domain is $[0, 1]$ and the discontinuity is initially located at x_0 and t_{end} is the final time. The computations are performed on 1000 grid points and the CFL condition is 0.5. The initial condition and the physical parameters of the test cases are described on Table 1 (p denote the pressure and $\mathcal{T} = -pI$ at initial time).

The test case TC1 is the classical Sod gas shock tube. An interface separates two chambers with different pressure and density. The solution in the physical domain is shown in Figure 2. The results compare well with the literature.

The test case TC2 is a copper shock tube with shear. An interface separates the high pressure chamber on the left where the copper is at rest and the same material on the right at low pressure. Also a tangential velocity discontinuity

is imposed on the right. The results for the pressure in the physical domain are shown in Figure 3. We have five waves in the field, the pressure is discontinuous at the contact discontinuity. These results compare well with those presented in [2] and [3].

The last test case is the same as TC2 but the initial discontinuity is along the line $x + y = 1$. The numerical domain is $[0, 1]^2$ and the computations are performed on a 500×500 cartesian mesh with a 0.5 CFL condition. The results for the pressure in the physical domain are shown in Figure 4. The results compare well with the solution of Figure 3. However we can see that the pressure is diffuse at the contact discontinuity.

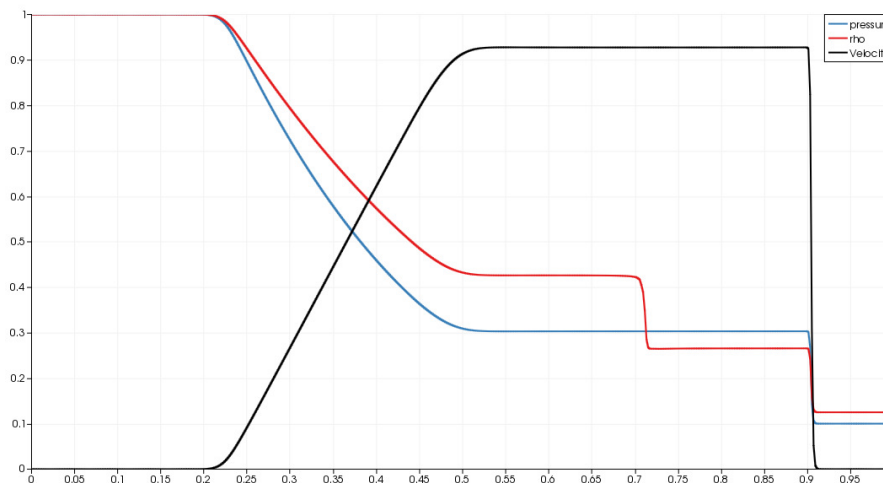| TC	side	ρ_0	u_1	u_2	p	γ	p_∞	χ	x_0	t_{end}
1	left	1	0	0	1	1.4	0	0	0.5	0.22
	right	0.125	0	0	0.1	1.4	0	0		
2	left	8900	0	0	10^9	4.22	$3.42 \cdot 10^{10}$	$5 \cdot 10^{10}$	0.5	$5\ 10^{-5}$
	right	8900	0	100	10^5	4.22	$3.42 \cdot 10^{10}$	$5 \cdot 10^{10}$		

Table 1: One-dimensional test case description.

Figure 2: TC1. Plot of pressure, density and normal velocity in the physical domain at $t = 0.22s$

5 CONCLUSIONS

We have synthetically presented a model to deal with compressible multimaterials in the Lagrangian framework. We show 1D validations test cases of gas-gas and elastic-elastic interaction. Ongoing research adresses 2D simulations and air-elastic interaction.

REFERENCES

[1] S.K Godunov. Elements of continuum mechanics. Nauka Moskow. 1978.

[2] N. Favrie and S.L. Gavrilyuk and R. Saurel. Solid-fluid diffuse interface model in cases of extreme deformations. *Journal of Computational Physics*, 228(16), 6037-6077, 2009.

[3] A. Iollo, T. Milcent, H. Telib. A sharp contact discontinuity scheme for multimaterial models. *Finite Volumes for Complex Applications VI*. Springer Proceedings in Mathematics 4, 2011.

[4] Y. Gorsse, A. Iollo, T. Milcent, H. Telib. Accurate sharp interface scheme for multimaterial. *International Conference on Computational Fluid Dynamics (ICCFD7)*. Hawaii, 2012.

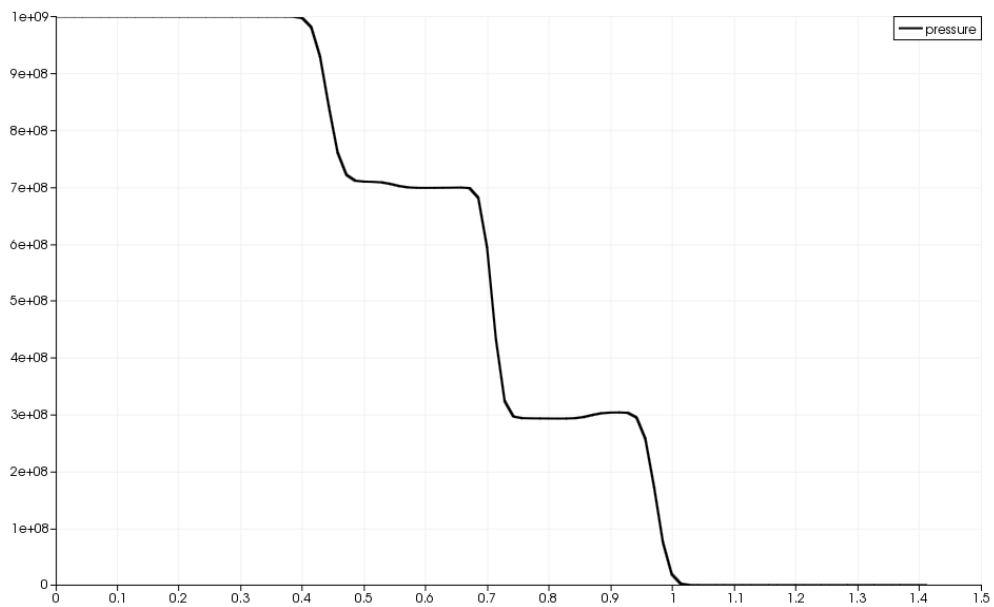Figure 3: TC2. Plot of pressure in the physical domain at $t = 5 \ 10^{-5} s$

Figure 4: TC3. Plot of pressure in the physical domain at $t = 5 \ 10^{-5} s$